Are Buckminsterfullerenes Molecular Ball Bearings?

Romain Lhermerout, Christophe Diederichs, Sapna Sinha, Kyriakos Porfyrakis, Susan Perkin

Are Buckminsterfullerenes "Molecular Ball Bearings"?

Romain Lhermerout,[†] Christophe Diederichs,[†] Sapna Sinha,[‡] Kyriakos Porfyrakis,[‡] and Susan Perkin*,[†]

†*Department of Chemistry, Physical and Theoretical Chemistry Laboratory, University of Oxford, Oxford OX1 3QZ, UK*
‡*Department of Materials, University of Oxford, Parks Road, Oxford OX1 3PH, UK*

E-mail: susan.perkin@chem.ox.ac.uk

Abstract

Buckminsterfullerenes (C_{60}) are near-spherical molecules which freely rotate at room temperature in the solid state and when dissolved in solution. An intriguing question arises as to whether C_{60} molecules can act as "molecular ball bearings", i.e. preventing direct contact between two solid surfaces whilst simultaneously dissipating shear stress through fast rotation. To explore this, we performed measurements of friction across a solution of C_{60} in the boundary lubrication regime. High resolution shear and normal force measurements between mica sheets separated by the C_{60} solution were made using a Surface Force Balance to provide a single-asperity contact and sub-nanometer resolution in film thickness. We find that, even at small volume fraction, C_{60} forms a solid-like amorphous boundary film sustaining high normal load, suggesting that this system undergoes a glass transition under confinement. The C_{60} film gives rise to a low friction coefficient up to moderate applied loads, and we discuss the possible relevance of the ball bearing effect at the molecular scale.

Introduction

Human activity has always required the motion of objects, from the building of edifices in prehistorical ages to the harvesting of energy with wind turbines in present times. The question of whether logs were used as "rollers" to move megaliths has been debated,[1] nonetheless it is clear that the idea of using wheels to replace sliding by rolling was early found to be an efficient way to reduce energy dissipation during motion, i.e. friction. While formulating the first fundamental laws of solid friction, Da Vinci conceived of many ingenious machines involving rotary parts where the friction is limited to the axis.[2] Ball bearings, consisting of balls running along a groove (e.g. in an axle assembly), are designed to reduce the friction further by transforming sliding into rolling. It is also known, since ancient times,[3] that lubricating the contact, i.e. inserting a liquid between the moving solids, is an efficient way to reduce wear and produce a moderate, or at least stable friction. However, finding good lubricants is complex because the appropriate mixture has to remain effective in harsh conditions (high loads/shear stresses/temperatures, humidity etc.), and the field of tribology has been active over the past century and until today.[4–6] Detailed, mechanistic interpretations of friction are often complicated by processes acting over multiple length-scales and timescales simultaneously. For example a fluid may lubricate motion as a thick film (hydrodynamic regime) or in molecular confinement between close asperities (boundary regime), either at dif-

ferent regions of a rough contact or under different shearing conditions.

Buckminsterfullerene (C_{60}) is a molecule of almost ideal spherical shape[7] (structure in Figure 1(a)). In its pure form under ambient conditions C_{60} forms a solid in which the molecules are able to rotate freely; inspection of the temperature dependence of the heat capacity shows that the energy associated with rotation of C_{60} in the crystal is smaller than the ambient thermal energy.[8] This interesting property, combined with relative chemical stability, led to the early proposal that C_{60} could act as an effective boundary lubricant: it might be expected that even when confined between two surfaces it could rotate to dissipate stress, the molecules effectively performing as "molecular ball bearings". Direct observations have shown that spherical nanoparticles can rotate between sheared surfaces, in a manner which is reminiscent of the rolling without slipping motion of macroscopic ball bearings.[9] By analogy to the macroscopic mechanism of ball bearings, a molecular ball bearing system should sustain normal load (i.e. keeping the shearing solid surfaces apart) yet without hindering molecular rotations (which serve to dissipate shear stress and so reduce friction). Although this provides a useful motivating concept to consider the effect of rotations in modifying friction at the nanoscale, we note that the macroscopic mechanism of ball bearings does not map perfectly onto molecular systems under ambient conditions: the molecular rotation rate will typically be much higher than the imposed shear under ambient conditions. To differentiate between these two situations, we call the molecular mechanism the "molecular ball bearing effect". In this work we measure and appraise whether C60 might satisfy these criteria.

Previous studies have investigated lubrication by C_{60} or fullerene-like molecules in different ways. On one hand, they have been used as a solid lubricant in dry conditions (from simply dispersed powder to carefully sublimated thin film), but they didn't provide particularly exceptional frictional properties.[10–14] C_{60} have been used as wheels for single-molecule "nanocars", and the displacement of such nanocars was found to be indeed due to the rotation of the C_{60} on the Au-(111) surface at $\sim$ 200 °C.[15] Experimental and numerical studies investigated the frictional behavior on a C_{60} single crystal around an orientational order-disorder phase transition at $\sim$ 260 K, but no significant change of friction coefficient was found.[16,17] On the other hand, when C_{60} or fullerene-like molecules have been used as an additive in a liquid, they formed a protective boundary film that prevents wear and induces a stable frictional response.[18–20] In particular, Campbell et al. confined a dispersion of C_{60} in toluene between atomically-smooth mica surfaces in a Surface Force Apparatus, and studied the hydrodynamic lubrication regime by looking at the viscous response to a normal oscillation. They showed that this system exhibits a full slip boundary condition, suggesting a particular "fluidity" of the C_{60} that are adsorbed on the surfaces.[18] In the present paper, we report the first measurements of friction across a dispersion of C_{60} in the boundary lubrication regime.

Methods

Materials. C_{60} was synthesised via the arc discharge method according to the procedure first published by Krätschmer et al.[21] and was further isolated by high performance liquid chromatography (HPLC) to a purity of 99.5%. Tetralin, 1,2,3,4-tetrahydronaphthalene (Sigma-Aldrich, anhydrous, 99%), was used as solvent (chemical structure in Figure 1(a)). Tetralin was chosen as a good solvent for C_{60} (solubility of C_{60} in tetralin is 16 mg/mL at 25 °C[22]) with low volatility (vapor pressure of 0.05 kPa at 25 °C[23]) and a moderate viscosity (2.015 mPa.s at 25 °C[24]). The tetralin was dried with molecular sieves (0.4 nm pore size, from Fisher Chemical) for a week, and filtered before use (Ultra-Cruz Syringe Filter, PTFE, 0.22 μm). C_{60} molecules were dispersed at a concentration of 5.60 $\pm$ 0.01 mg/mL, corresponding to a molar fraction of 0.1065 $\pm$ 0.0002% (given the tetralin density of 0.9645 g/mL at 25 °C[23]), or

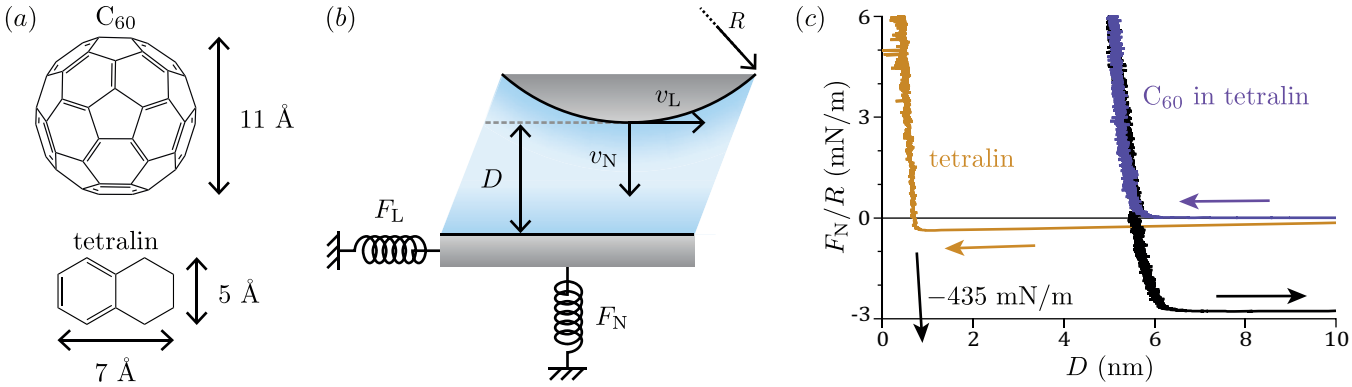

Figure 1: (a) Chemical structures and sizes of buckminsterfullerene (C_{60}) and tetralin. (b) Schematic of the SFB experiment, that allows to determine the interaction and friction forces between two mica surfaces separated by a liquid film of controlled thickness. (c) Normal force F_N rescaled by the radius of curvature R of the surfaces as a function of the separation D obtained at approach velocities $v_N \sim 1$ nm/s, for tetralin (approach in brown, pull-off force measured on retraction indicated by the black arrow) and the solution of C60 in tetralin (approach in purple, retraction in black).

a mean distance between the C_{60} molecules of 5.979 ± 0.004 nm $\sim 5 \times$ (C_{60} diameter).

Force measurements. The measurements were performed with a Surface Force Balance (SFB), which is a method ideal for the study of normal and lateral forces transmitted across fluid and soft films with high resolution. A schematic diagram of the key aspects is in Figure 1(b). The liquid film is held between two optical lenses, hemi-cylindrical in shape (radius of curvature $R \sim 1$ cm) and arranged in crossed-cylinder configuration. This geometry provides a point of closest approach between the two surfaces, which is model experiment for study of a single-asperity contact. The optical lenses are coated with single crystal sheets of mica, so that the roughness is sub-molecular (roughness arising only from the atomic corrugation of the crystalline surfaces). The precise geometry and liquid thickness are measured directly in-situ using white light interferometry; so-called Fringes of Equal Chromatic Order (FECO). The surfaces (lenses) can be translated in both normal and lateral directions relative to one another, and the resulting forces between them are detected via the deflection of normal and lateral springs. These measurements can be performed simultaneously, so that information about film thickness, normal force, and shear force can be measured in parallel (e.g. during approach of the surface from large distances to contact). The details of the procedure have explained elsewhere;[25–28] in the following we note the quantities and details particular to the present experiments.

Muscovite mica is cleaved, backsilvered and glued on glass cylindrical lenses using dextrose, D-(+)-glucose (Sigma-Aldrich, 99.5%, chosen for its insolubility in tetralin). Two surfaces are mounted in a crossed-cylinder geometry to make a single contact between atomically smooth surfaces, and the liquid is injected in between to form a capillary bridge. The chamber is dried with P_2O_5, phosphorus pentoxide (Sigma-Aldrich, 99%) and the room is regulated to 25°C. FECO are analyzed to measure the radius of curvature R of the surfaces and the liquid thickness, D. D is measured with a precision of 0.02 nm (RMS noise) and accuracy of 1 nm and $D = 0$ is defined as the mica-mica contact position measured in dry air before liquid injection. The refractive indeces of 1.5413 at 20°C for tetralin[23] and 1.5417 at 22°C for the mixture were measured with a Bellingham+ Stanley Abbe 60 ED refractometer.[29] A stepper motor is used to approach or retract the top surface at a normal velocity v_N and a sectored piezo-electric tube allows application of

a shearing motion at lateral velocity v_L. Normal force F_N and lateral force F_L are then measured using springs, with respective stiffness of 133.8 ± 3.0 N/m and 441 ± 4 N/m.

Results

Normal force. The normal force profiles obtained are shown in Figure 1(c). For pure tetralin, the surfaces experience a (van der Waals) attractive interaction on approach of the surfaces to $\sim$ 10 nm causing a jump-in to contact. The surface separation just after the jump-in is close to the direct mica-mica contact value (within the systematic experimental error). The finite gradient of this soft wall is due to the compression of the mica, the single material remaining in the optical interferometer. On retraction the two surfaces jump-out when reaching a pull-off force of $F_{adh}/R = -435$ mN/m, which according to the JKR theory corresponds to an adhesion energy of $W = 2F_{adh}/(3\pi R) = -92$ mN/m.[25] This value is comparable with the adhesion energy between -160 mN/m and -108 mN/m measured previously for mica-mica contact in dry nitrogen.[30] It is not clear why a structural force is not observed in this case, as might be expected by comparison with similar measurements with apolar liquids like cyclohexane, benzene or toluene which do each give rise oscillatory structural surface forces .[26,31–35] However, a similarly strong adhesion minimum has also been observed for these liquids, and attributed to the presence of traces of water that wets the mica surfaces. Particular care was taken to use tetralin in dry conditions (storage in molecular sieves, measurements with P_2O_5 in the chamber), however it is still possible that traces of water may remain giving rise to an adsorbed layer or part-layer on the mica. In the subsequent experiments we take this control measurement with pure tetralin as the reference situation in order to investigate the effect of the addition of small quantities of C_{60} under the same conditions.

When 0.1 mol % C_{60} is added to the tetralin the normal force between the surfaces is modified significantly, as clear in Figure 1(c). On approach of the surfaces a repulsive soft wall is reached at $\sim$ 6 nm, compressing by several nm with increased load (appearing even more clearly in Figure 3(b)). The onset of repulsion corresponds to the thickness of approximately 5 C_{60} molecules, and the soft wall holds for loads up to 80 μN, corresponding to a pressure of $\sim$ 6 MPa (given the contact radius of $\sim$ 2 μm), and on retraction an adhesive minimum of $F_{adh}/R = -2.7$ mN/m is obtained. This value is comparable with what Campbell et al. measured for C_{60} in toluene between mica.[18]

In summary of the normal force profiles, we find that very small volume fractions of C_{60} lead to substantial modification to the interaction force between confining surfaces, giving rise to a monotonic repulsive force extending to $\sim$ 5 molecular diameters. This insight allows us subsequently to interpret the direct friction measurements, as follows.

Lateral force. Having characterised the normal interaction between the surfaces, we next applied a lateral (shearing) motion of the top surface relative to the bottom surface and detected the resulting lateral force transmitted across the liquid. In the SFB this can be performed at the same time as approaching the surfaces and measuring the film thickness and normal force; in this section we present results of the measured friction as a function of separation and load. We compare the case of pure tetralin, as control, to the tetralin with C_{60}. In Figure 2 we show the result of measurements with pure tetralin (part (a)) and with C_{60} in tetralin (part(b)). For the control experiment with pure tetralin, we show the temporal evolution of the liquid thickness D and the lateral force F_L when the top surface is moved downward and then upward at $v_N = 0.92 \pm 0.05$ nm/s and simultaneously oscillated laterally at $v_L = 287 \pm 1$ nm/s. When the surfaces are separated by a finite film of tetralin, before reaching surface contact, no measurable lateral force is detected (smaller than the sensitivity of ~ 1 μN), meaning there is no mechanical coupling between the surfaces. At the point of jump-in to contact the lateral force instantaneously increases

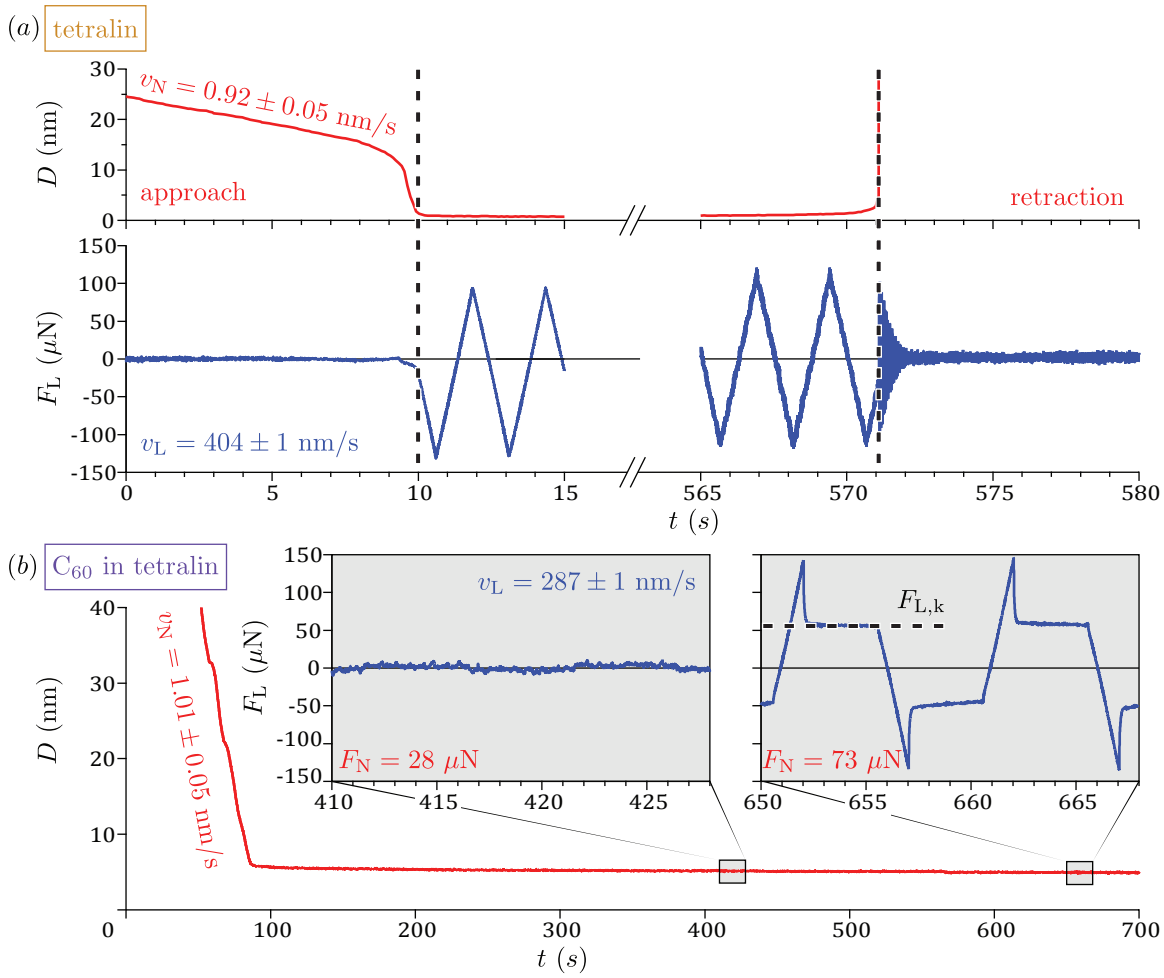

Figure 2: (a) Temporal evolutions of liquid thickness D (red traces) and lateral force F_L (blue traces) when approaching and retracting mica surfaces separated by tetralin with simultaneous constant-velocity shearing of one surface. The lateral force is below the experimental resolution until the surfaces reach direct contact, at which point they are rigidly coupled. (b) Temporal evolution of liquid thickness D when approaching the surfaces and simultaneously applying constant-velocity lateral motion to one surface across the solution of C_{60} in tetralin. The insets show the lateral force F_L at two time intervals (or equivalently two loads F_N as indicated), showing how the lateral force during shearing cycles evolves as the applied load is increased. At higher loads a clear yield spike followed by smooth sliding is observed; from this the kinetic friction $F_{L,k}$ is deduced.

in magnitude and varies directly with the applied shearing amplitude; the saw-tooth shape is the signature that the surfaces are rigidly coupled, i.e with no relative motion throughout the cycle. Because of the strong adhesion between the surfaces, friction is controlled by adhesion[36] and is so high that the yield point of the contact is not reached within the range of lateral force explored. Thus we find that the yield force of the contact must be higher than 110 μN in this case. In experiments with higher shearing amplitudes, we found that the yield force was in fact higher than 330 μN; corresponding to a lower limit for the contact shear stress of $\sigma_{\mathrm{L}} \sim 26$ MPa. During retraction, a damped oscillation at the resonance frequency of ~ 25 Hz is obtained when the surfaces jump-out, and then no lateral force is detected, consistently with the behavior on approach. In sum, we find that tetralin alone cannot support any applied load, and so squeezes out of a contact when finite load is applied, giving rise to high friction in accordance with direct mica-mica contact.

Lateral forces measured across the solution of C_{60} in tetralin as a function of load - examples of which are in Figure 2(b) - show an entirely different behavior. When the surfaces approach to the distance corresponding to the repulsive wall the lateral force is still below the sensitivity limit. It was necessary to increase the load before any detectable lateral force could be recorded between the surfaces; the left-hand inset show the emergence of tiny lateral forces when the surfaces are being pushed together with a force of 28 μN. The amplitude of the lateral force then increases with the load, and the signal exhibit a strong stiction spike followed by a plateau (right-hand side inset). The clear yield point followed by sliding behavior is typical of a solid-like response to lateral applied stress. We systematically extracted the amplitude of the plateau, which we identified as the kinetic friction force $F_{\mathrm{L,k}}$. In Figure 3(b) we compare the normal force and kinetic friction force profiles as a function of surface separation, D. In this representation, we clearly see that the range of the friction force is much smaller than the range of the normal force, becoming measurable only at separations of ~ 4 nm at which point the layer is already substantially compressed and the load is high, qualitatively similar to what has been observed for lubrication by polymer brushes.[37] As shown in Figure 3(a), the relationship between the kinetic friction force and the load is not linear, instead it has a strongly convex shape. At small loads, kinetic friction is proportional to the load, with no significant contribution from adhesion (zero friction at zero imposed load) and a coefficient of proportionality $\mu = 0.072 \pm 0.002$ (with the coefficient of friction defined as the local slope $\mu = \mathrm{d}F_{\mathrm{L,k}}/\mathrm{d}F_{\mathrm{N}}$). This quantity increases with the load, and reaches $\mu = 4.1 \pm 1.6$ at the maximum imposed load. Thus the friction coefficient evolves from a very low value, indicating efficient lubrication at moderate load, up to a high value under strong compression. To comment on these values, it is useful to compare them to the friction coefficient of different liquids between mica surfaces, all measured with a Surface Force Balance. Simple apolar liquids are generally characterized by a single friction coefficient: 1.1 for octamethylcyclotetrasiloxan (OMCTS), 2.2 for cyclohexane.[38] Ionic liquids exhibit quantized friction,[39] i.e. a friction coefficient indexed by the number of ordered layers of ions in the film, typically varying from 0.007 to 0.5 for 1-decyl-1-methylpyrrolidinium bis[(trifluoromethane)sulfonyl]imide, [$C_{10}C_1$Pyrr][NTf_2].[40] Regarding the low-load friction coefficient, the C_{60} solution is thus between apolar liquids and ionic liquids, and is comparable with the 0.12 obtained for 2,6,10,15,19,23-hexamethyltetracosane (squalane), a branched hydrocarbon liquid that has been reported for exhibiting glassy behavior in certain confinement conditions.[41]

Discussion

A solid film. We now propose a simple qualitative picture of what is happening at the molecular scale to interpret the observed behavior. The molecular forces governing the interaction between C_{60}, tetralin and mica include van des Waals and steric forces. Mica is polar, and maybe covered with a (sub-)molecular

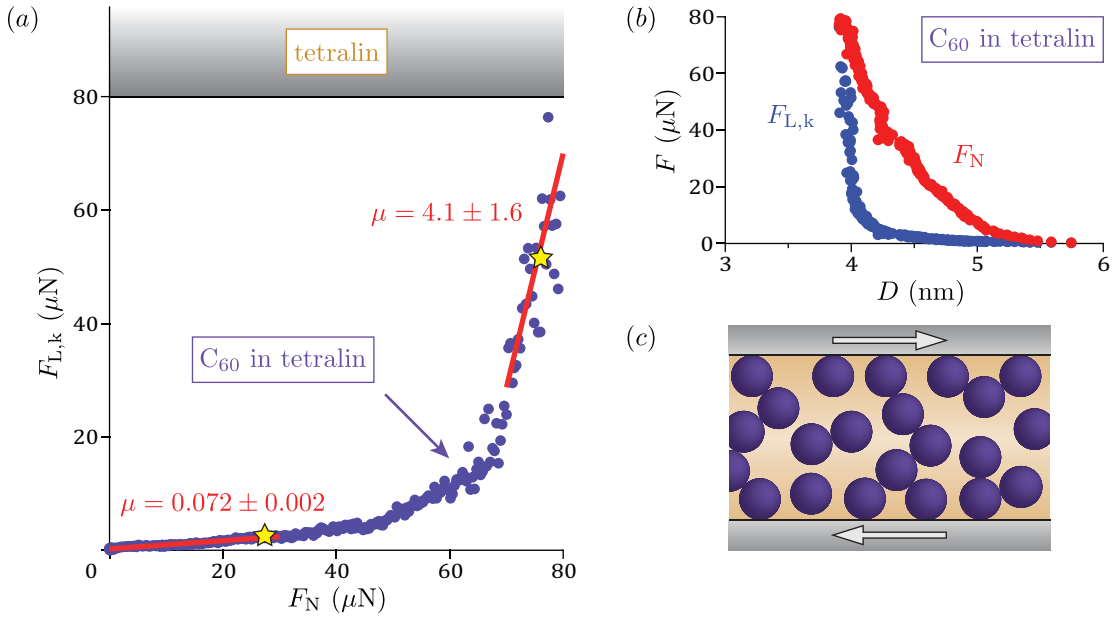

Figure 3: (a) Kinetic friction $F_{L,k}$ as a function of load F_N. Friction in pure tetralin was above the range limit of the experiment, as indicated by the shaded bar, whereas the solution of C_{60} in tetralin gave rise to measurable friction (in purple). The two stars correspond to the lateral force traces shown in insets of Figure 2(b), and the red lines are the linear fits used to deduce the local friction coefficient μ. (b) Normal (red) and kinetic friction (blue) force profiles, for the solution of C_{60} in tetralin. (c) Schematic representation of the system in confinement: the C_{60} molecules are randomly packed, steric interactions lead to a significant repulsion between the solid surfaces, but fast rearrangements induce a relatively small shearing resistance.

film of water. Tetralin is slightly polar and polarizable (calculated static polarizability of 1.8×10^{-39} C $\cdot$ m^2/V), whereas C_{60} is more polarizable because of the highly delocalized π electrons (measured static polarizability of 8.6×10^{-39} C $\cdot$ m^2/V[42]). When the mica surfaces are far apart, the C_{60} molecules in the bulk are separated by an average distance of about 5 times their diameter (deduced from the chosen concentration) and are attracted by a dispersion (London) interaction but the liquid dispersion is thermodynamically stable because the concentration is (just) below the saturation limit. A monolayer of C_{60} is probably initially adsorbed on each mica surface due to the induction (Debye) interaction and the preference of mica for the more polar C_{60} rather than tetralin. When confining the liquid, tetralin tends to be squeezed-out, as shown by the reference measurement. The local concentration of C_{60} in the gap therefore increases as the surfaces approach and the C_{60} molecules - which are already close to the aggregation limit in the bulk solution - are expected to agglomerate, forming a strongly bound solid film (as shown by the soft wall in the normal force profile). The fact that this film holds for pressures up to ~ 6 MPa is remarkable, given that a yield stress of about ~ 1 MPa is measured when compressing a C_{60} single crystal along the $\langle 1\,1\,0 \rangle$ direction.[43] This is probably due to the fact that we are dealing with a nanometric film, the C_{60} having attractive interactions with the confining surfaces and being packed in a disordered arrangement with no cleaving plane.

A disordered film. The absence of order in the film is revealed by the normal force profile showing a soft wall at distance of approximately 5 C_{60} diameters. This behavior was unexpected, because a structural force is usually observed for apolar liquids between mica. When Campbell et al. studied a solution of C_{60} in toluene between mica, they observed a soft wall at $\sim$ 3.4 nm at approach velocities higher than 5 nm/s, or a structural force of period of 1.1 nm equal to the diameter of the C_{60} molecules at smaller velocities.[18] They interpret this transition as C_{60} molecules being kinetically trapped between the surfaces and having no time to order. We never observed a structural force over the explored spots on the surfaces, experiments and velocities between $\sim$ 1 nm/s and $\sim$ 12 nm/s. This is most likely to be due to the different solvent and concentration chosen: Campbell et al. used a concentration of 0.095 mg/mL corresponding to a molar fraction of $\sim 0.001\%$ or $\sim 3\%$ of the saturation limit in toluene (2.8 mg/mL at 25 °C[22]), whereas here we use a concentration of 5.60 mg/mL corresponding to a molar fraction of $\sim 0.1\%$ or $\sim 35\%$ of the saturation limit in tetralin (16 mg/mL at 25 °C[22]). In our case, the C_{60} molecules in the bulk are much more concentrated and close to the agglomeration limit, and the order/disorder kinetic transition may have been shifted to approach velocities much smaller than 1 nm/s. Combining the observations of no structural force and of a solid-like friction response, we conclude that under the experimental conditions used the C_{60} must form a disordered/amorphous solid, i.e. a glass, where the molecules are randomly packed in the gap (as illustrated in Figure 3(c)). The situation is thus related to the difficult problem of glass transition in confinement, already investigated for various systems[44] like simple liquids,[45] polymers,[46] liquid crystals[47] or colloids.[48] It is then tempting to interpret our measured kinetic friction-load curve as a kind of Angell plot, that conventionally represents how the logarithm of the viscosity increases with the inverse temperature (for molecular liquids) or with the packing fraction (for colloidal liquids) when approaching the glass transition.[49,50] Following this scenario, it would be the increase of the C_{60} packing fraction with the load (as shown by the compression of the film) that leads to a dramatic slowing down of the dynamics, i.e. of the rearrangement timescale of the glassy film in the gap, as measured by the increase of the friction force.

Role of rotation. One can finally ask whether the rotation of C_{60} contributes to the frictional behavior. As shown by a 2D molecular dynamics simulation of lubrication by circular molecules, a high concentration in the gap can lead to jamming, which hinders the molecular rotation because the two sides of two

molecules in contact would have to rotate in opposite directions.[51] So if the rotation of C_{60} plays a role in our system, it is likely to happen at small loads, for which we indeed measured a small friction coefficient. Because of the relatively strong adhesion of the C_{60} on mica (Debye interaction), the lateral motion is probably distributed in the middle of the gap and not at the film/mica interfaces. The small resistance to flow in the gap indicates that energy is dissipated efficiently in the film; the mechanism for this could originate from (at least) three modes. First, there is only small adhesion between C_{60} molecules (London interaction).[18] Second, there is room and time for rearrangements, since C_{60} molecules are randomly packed with vacancies, at a packing fraction far enough from the glass transition. Third, the C_{60} may rotate freely in the thin disordered film, like they do in the bulk crystal, and this free rotation could contribute to a dissipation mechanism leading to low friction. In other words, a "molecular ball bearing" effect may be occurring and be partly responsible for the low friction regime.

Conclusions

To summarize our findings, C_{60} performs as an excellent boundary lubricant additive in our system; $\sim 0.1\%$ of C_{60} is sufficient to form a strong boundary film that reduces wear by preventing direct contact between the sliding surfaces and gives rise to a small friction coefficient at moderate loads. A key ingredient leading to this useful outcome is that C_{60} has a finite solubility and tends to solidify when the concentration exceeds the saturation point locally in confined contacts thus preventing squeeze-out of the film. The fact that the C_{60} appears to form a disordered solid, evidenced by no regular oscillatory structural force despite solid-like mechanical response, indicates that the convex friction-load relationship may be the manifestation of a glass transition under confinement. The friction coefficient at moderate loads is remarkably small, and so it is hypothesised that the molecular rotations intrinsic to C_{60} – the "molecular ball bearing effect" – may be important for reducing shear stress.

Future investigations should involve a systematic study of the effect of the concentration on kinetic trapping and on friction response. To clarify the role of molecular rotation, comparative Surface Force Balance measurements with C_{60} chemically grafted to the surfaces and thus unable to rotate[52,53] could be performed. It would also be of interest to study different surface materials such as graphene;[54] with only sp^2-hybridized carbon materials exceptional properties can emerge.[55–57]

Author Contributions

R.L. and C.D. performed the experiments. S.P. and R.L. conceived of the project, interpreted the data and wrote the paper. K.P. and S.S. synthesised the fullerenes and contributed to the experimental design.

Acknowledgement S.P. and R.L. are supported The Leverhulme Trust (RPG-2015-328) and the ERC (under Starting Grant No. 676861, LIQUISWITCH). R.L. is supported by the EPA Cephalosporin Junior Research Fellowship and Linacre College (University of Oxford). S.P. is grateful for research leave enabled by the Philip Leverhulme Prize.

References

(1) Richards, J.; Whitby, M. In *Science and Stonehenge*; Cunliffe, B., Renfrew, C., Eds.; British Academy, 1997; pp 231–256.

(2) Hutchings, I. M. Leonardo da Vinci's Studies of Friction. *Wear* **2016**, *360-361*, 51 – 66.

(3) Fall, A.; Weber, B.; Pakpour, M.; Lenoir, N.; Shahidzadeh, N.; Fiscina, J.; Wagner, C.; Bonn, D. Sliding Friction on Wet and Dry Sand. *Phys. Rev. Lett.* **2014**, *112*, 175502.

(4) Bowden, F. P.; Tabor, D. *The Friction and Lubrication of Solids*; Oxford University Press, 1950.

(5) Urbakh, M.; Klafter, J.; Gourdon, D.; Israelachvili, J. The Nonlinear Nature of Friction. *Nature* **2004**, *430*, 525.

(6) Lhermerout, R.; Diederichs, C.; Perkin, S. Are Ionic Liquids Good Boundary Lubricants? A Molecular Perspective. *Lubricants* **2018**, *6*.

(7) Kroto, H. W.; Heath, J. R.; O'Brien, S. C.; Curl, R. F.; Smalley, R. E. C_{60}: Buckminsterfullerene. *Nature* **1985**, *318*, 162.

(8) Bagatskii, M. I.; Sumarokov, V. V.; Barabashko, M. S.; Dolbin, A. V.; Sundqvist, B. The Low-Temperature Heat Capacity of Fullerite C_{60}. *Low Temp. Phys.* **2015**, *41*, 630–636.

(9) Lahouij, I.; Dassenoy, F.; Vacher, B.; Martin, J.-M. Real Time TEM Imaging of Compression and Shear of Single Fullerene-Like MoS_2 Nanoparticle. *Tribol. Lett.* **2012**, *45*, 131–141.

(10) Blau, P. J.; Haberlin, C. E. An Investigation of the Microfrictional Behavior of C_{60} Particle Layers on Aluminum. *Thin Solid Films* **1992**, *219*, 129 – 134.

(11) Thundat, T.; Warmack, R. J.; Ding, D.; Compton, R. N. Atomic Force Microscope Investigation of C_{60} Adsorbed on Silicon and Mica. *Appl. Phys. Lett.* **1993**, *63*, 891–893.

(12) Bhushan, B.; Gupta, B. K. Friction and Wear of Ion-Implanted Diamondlike Carbon and Fullerene Films for Thin-Film Rigid Disks. *J. Appl. Phys.* **1994**, *75*, 6156–6158.

(13) Lüthi, R.; Meyer, E.; Haefke, H.; Howald, L.; Gutmannsbauer, W.; Guggisberg, M.; Bammerlin, M.; Güntherodt, H.-J. Nanotribology: an UHV-SFM Study on Thin Films of C_{60} and AgBr. *Surf. Sci.* **1995**, *338*, 247 – 260.

(14) Luengo, G.; Campbell, S. E.; Srdanov, V. I.; Wudl, F.; Israelachvili, J. N. Direct Measurement of the Adhesion and Friction of Smooth C_{60} Surfaces. *Chem. Mater.* **1997**, *9*, 1166–1171.

(15) Shirai, Y.; Osgood, A. J.; Zhao, Y.; Kelly, K. F.; Tour, J. M. Directional Control in Thermally Driven Single-Molecule Nanocars. *Nano Lett.* **2005**, *5*, 2330–2334.

(16) Liang, Q.; Tsui, O. K. C.; Xu, Y.; Li, H.; Xiao, X. Effect of C_{60} Molecular Rotation on Nanotribology. *Phys. Rev. Lett.* **2003**, *90*, 146102.

(17) Benassi, A.; Vanossi, A.; Pignedoli, C. A.; Passerone, D.; Tosatti, E. Does Rotational Melting Make Molecular Crystal Surfaces More Slippery? *Nanoscale* **2014**, *6*, 13163–13168.

(18) Campbell, S. E.; Luengo, G.; Srdanov, V. I.; Wudl, F.; Israelachvili, J. N. Very Low Viscosity at the Solid-Liquid Interface Induced by Adsorbed C_{60} Monolayers. *Nature* **1996**, *382*, 520.

(19) Golan, Y.; Drummond, C.; Homyonfer, M.; Feldman, Y.; Tenne, R.; Israelachvili, J. Microtribology and Direct Force Measurement of WS_2 Nested Fullerene-Like Nanostructures. *Adv. Mater.* **1999**, *11*, 934–937.

(20) Drummond, C.; Alcantar, N.; Israelachvili, J.; Tenne, R.; Golan, Y. Microtribology and Friction-Induced Material Transfer in WS_2 Nanoparticle Additives. *Adv. Funct. Mater.* **2001**, *11*, 348–354.

(21) Krätschmer, W.; Lamb, L. D.; Fostiropoulos, K.; Huffman, D. R. Solid C_{60}: A New Form of Carbon. *Nature* **1990**, *347*, 354.

(22) Ruoff, R. S.; Tse, D. S.; Malhotra, R.; Lorents, D. C. Solubility of C_{60} in a Variety of Solvents. *J. Phys. Chem.* **1993**, *97*, 3379–3383.

(23) Lide, D. R. *CRC Handbook of Chemistry and Physics, 90th Edition (CD-ROM Version 2010)*; CRC Press, 2010.

(24) Gonçalves, F. A.; Hamano, K.; Sengers, J. V. Density and Viscosity of Tetralin and *Trans*-Decalin. *Int. J. Thermophys.* **1989**, *10*, 845–856.

(25) Israelachvili, J. N. *Intermolecular and Surface Forces (Third Edition)*; Academic Press, 2011.

(26) Klein, J.; Kumacheva, E. Simple Liquids Confined to Molecularly Thin Layers. I. Confinement-Induced Liquid-to-Solid Phase Transitions. *J. Chem. Phys.* **1998**, *108*, 6996–7009.

(27) Perkin, S.; Chai, L.; Kampf, N.; Raviv, U.; Briscoe, W.; Dunlop, I.; Titmuss, S.; Seo, M.; Kumacheva, E.; Klein, J. Forces Between Mica Surfaces, Prepared in Different Ways, Across Aqueous and Non-aqueous Liquids Confined to Molecularly Thin Films. *Langmuir* **2006**, *22*, 6142–6152.

(28) Lhermerout, R.; Perkin, S. Nanoconfined Ionic Liquids: Disentangling Electrostatic and Viscous Forces. *Phys. Rev. Fluids* **2018**, *3*, 014201.

(29) Israelachvili, J. N. Thin Film Studies Using Multiple-Beam Interferometry. *J. Colloid Interface Sci.* **1973**, *44*, 259 – 272.

(30) Horn, R. G.; Israelachvili, J. N.; Pribac, F. Measurement of the Deformation and Adhesion of Solids in Contact. *J. Colloid Interface Sci.* **1987**, *115*, 480 – 492.

(31) Horn, R. G.; Israelachvili, J. N. Direct Measurement of Structural Forces Between Two Surfaces in a Nonpolar Liquid. *J. Chem. Phys.* **1981**, *75*, 1400–1411.

(32) Christenson, H. K.; Horn, R. G.; Israelachvili, J. N. Measurement of Forces Due to Structure in Hydrocarbon Liquids. *J. Colloid Interface Sci.* **1982**, *88*, 79 – 88.

(33) Christenson, H. K. Experimental Measurements of Solvation Forces in Nonpolar Liquids. *J. Chem. Phys.* **1983**, *78*, 6906–6913.

(34) Christenson, H. K.; Gruen, D. W. R.; Horn, R. G.; Israelachvili, J. N. Structuring in Liquid Alkanes Between Solid Surfaces: Force Measurements and Mean-Field Theory. *J. Chem. Phys.* **1987**, *87*, 1834–1841.

(35) Christenson, H. K.; Blom, C. E. Solvation Forces and Phase Separation of Water in a Thin Film of Nonpolar Liquid Between Mica Surfaces. *J. Chem. Phys.* **1987**, *86*, 419–424.

(36) Homola, A. M.; Israelachvili, J. N.; McGuiggan, P. M.; Gee, M. L. Fundamental Experimental Studies in Tribology: The Transition from "Interfacial" Friction of Undamaged Molecularly Smooth Surfaces to "Normal" Friction with Wear. *Wear* **1990**, *136*, 65 – 83.

(37) Klein, J.; Kumacheva, E.; Mahalu, D.; Perahia, D.; Fetters, L. J. Reduction of Frictional Forces Between Solid Surfaces Bearing Polymer Brushes. *Nature* **1994**, *370*, 634–636.

(38) Kumacheva, E.; Klein, J. Simple Liquids Confined to Molecularly Thin Layers. II. Shear and Frictional Behavior of Solidified Films. *J. Chem. Phys.* **1998**, *108*, 7010–7022.

(39) Smith, A. M.; Lovelock, K. R. J.; Gosvami, N. N.; Welton, T.; Perkin, S. Quantized Friction Across Ionic Liquid Thin Films. *Phys. Chem. Chem. Phys.* **2013**, *15*, 15317–15320.

(40) Smith, A. M.; Parkes, M. A.; Perkin, S. Molecular Friction Mechanisms Across Nanofilms of a Bilayer-Forming Ionic Liquid. *J. Phys. Chem. Lett.* **2014**, *5*, 4032–4037.

(41) Gourdon, D.; Israelachvili, J. N. Transitions Between Smooth and Complex Stick-Slip Sliding of Surfaces. *Phys. Rev. E* **2003**, *68*, 021602.

(42) Antoine, R.; Dugourd, P.; Rayane, D.; Benichou, E.; Broyer, M.; Chandezon, F.;

Guet, C. Direct Measurement of the Electric Polarizability of Isolated C_{60} Molecules. *J. Chem. Phys.* **1999**, *110*, 9771–9772.

(43) Fomenko, L.; Lubenets, S.; Izotov, A.; Nikolaev, R.; Sidorov, N. Mechanical Properties of C_{60} Single Crystals. *Mater. Sci. Eng. A.* **2005**, *400-401*, 320 – 324.

(44) Alba-Simionesco, C.; Coasne, B.; Dosseh, G.; Dudziak, G.; Gubbins, K. E.; Radhakrishnan, R.; Sliwinska-Bartkowiak, M. Effects of Confinement on Freezing and Melting. *J. Phys. Condens. Matter* **2006**, *18*, R15.

(45) Rosenhek-Goldian, I.; Kampf, N.; Yeredor, A.; Klein, J. On the Question of Whether Lubricants Fluidize in Stick-Slip Friction. *Proc. Natl. Acad. Sci. U.S.A.* **2015**, *112*, 7117–7122.

(46) Ellison, C. J.; Torkelson, J. M. The Distribution of Glass-Transition Temperatures in Nanoscopically Confined Glass Formers. *Nat. Mater.* **2003**, *2*, 695.

(47) Antelmi, D. A.; Kékicheff, P.; Richetti, P. The Confinement-Induced Sponge to Lamellar Phase Transition. *Langmuir* **1999**, *15*, 7774–7788.

(48) Leocmach, M.; Tanaka, H. Roles of Icosahedral and Crystal-Like Order in the Hard Spheres Glass Transition. *Nat. Commun.* **2012**, *3*, 974.

(49) Angell, C. A. Formation of Glasses from Liquids and Biopolymers. *Science* **1995**, *267*, 1924–1935.

(50) Royall, C. P.; Williams, S. R. The Role of Local Structure in Dynamical Arrest. *Phys. Rep.* **2015**, *560*, 1 – 75.

(51) Braun, O. M. Simple Model of Microscopic Rolling Friction. *Phys. Rev. Lett.* **2005**, *95*, 126104.

(52) Tsukruk, V. V.; Everson, M. P.; Lander, L. M.; Brittain, W. J. Nanotribological Properties of Composite Molecular Films: C_{60} Anchored to a Self-Assembled Monolayer. *Langmuir* **1996**, *12*, 3905–3911.

(53) Lee, S.; Shon, S., Y-S; Lee, T. R.; Parry, S. S. Structural Characterization and Frictional Properties of C_{60}-Terminated Self-Assembled Monolayers on Au(111). *Thin Solid Films* **2000**, *358*, 152 – 158.

(54) Britton, J.; Cousens, N. E. A.; Coles, S. W.; van Engers, C. D.; Babenko, V.; Murdock, A. T.; Koós, A.; Perkin, S.; Grobert, N. A Graphene Surface Force Balance. *Langmuir* **2014**, *30*, 11485–11492.

(55) Dienwiebel, M.; Verhoeven, G. S.; Pradeep, N.; Frenken, J. W. M.; Heimberg, J. A.; Zandbergen, H. W. Superlubricity of Graphite. *Phys. Rev. Lett.* **2004**, *92*, 126101.

(56) Miura, K.; Kamiya, S.; Sasaki, N. C_{60} Molecular Bearings. *Phys. Rev. Lett.* **2003**, *90*, 055509.

(57) Sasaki, N.; Itamura, N.; Miura, K. Atomic-Scale Ultralow Friction - Simulation of Superlubricity of C_{60} Molecular Bearing. *J. Phys. Conf. Ser.* **2007**, *89*, 012001.

Graphical TOC Entry